CrystEngComm

Accepted Manuscript

ROYAL SOCIETY OF CHEMISTRY

www.rsc.org/crystengcomm

A series of nine co-crystals formed from acridine and benzoic acids have been synthesized and structurally characterized and the influence of the halogen substituent on the formation of halogen and hydrogen bonding in co-crystals of title compounds has been investigated.

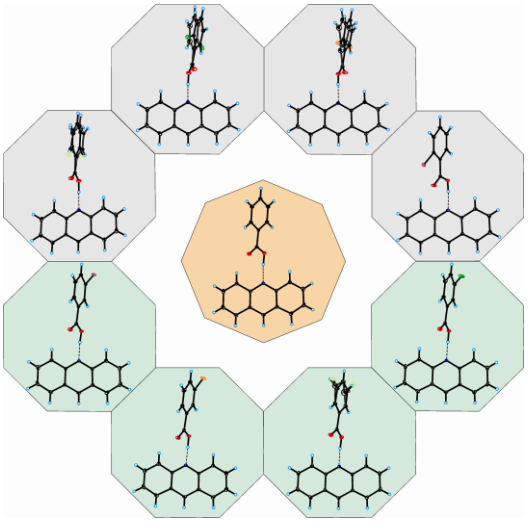

Cite this: DOI: 10.1039/c0xx00000x

www.rsc.org/xxxxxx

PAPER

Influence of the halogen substituent on the formation of halogen and hydrogen bonding in co-crystals formed from acridine and benzoic acids

Kornelia Kowalska, Damian Trzybiński and Artur Sikorski*

Received (in XXX, XXX) Xth XXXXXXXXX 20XX, Accepted Xth XXXXXXXXX 20XX

DOI: 10.1039/b000000x

In order to determine the influence of the *ortho*- and *meta*- halogen substituent in the phenyl ring of benzoic acid on the formation of C–H···X hydrogen bonds and X···O halogen bonds in crystal packing where the halogen (X) is a fluorine, chlorine, bromine or iodine atom, we synthesized and structurally characterized a series of nine co-crystals formed from acridine and benzoic acids: acridine • benzoic acid (**1**), acridine • 2-fluorobenzoic acid (**2**), acridine • 2-chlorobenzoic acid (**3**), acridine • 2-bromobenzoic acid (**4**), acridine • 2-iodobenzoic acid (**5**), acridine • 3-fluorobenzoic acid (**6**), acridine • 3-chlorobenzoic acid (**7**), acridine • 3-bromobenzoic acid (**8**) and acridine • 3-iodobenzoic acid (**9**). The number, type and strength of hydrogen bonds, halogen bonds and melting points of co-crystals **1**–**9** were compared. Systematic analysis of the intermolecular interactions taking place in the co-crystals of the title compounds indicates that competition between halogen and hydrogen bonding depends on the position and type of halo-substituent.

Introduction

Non-covalent interactions, such as hydrogen bonds, halogen bonds, C–H···π and π···π interactions, play a significant role in the self-assembly and molecular recognition processes of crystalline materials.[1] Recently, much attention has been focused on co-operation and competition between halogen and hydrogen bonds coexisting in the crystal packing of co-crystals, salts and solvates. A body of knowledge and an understanding of the geometry, energies and nature of these interactions has been acquired through systematic research published in the last ten years (some examples are listed below). Aakeröy and co-workers reported a supramolecular hierarchy among halogen-bond donors,[2a] demonstrated that an iodine-based halogen-bond donor can compete with a strong hydrogen-bond donor in crystals of five heteroaryl-2-imidazoles synthesized and co-crystallized with fifteen different halogen-bond donors,[2b] examined the non-covalent interactions in co-crystals of 3,3'-azobipyridine and 4,4'-azobipyridine with a series of bi-functional donor molecules including an activated halogen-bond donor,[2c] and discussed the structural competition between hydrogen bonds and halogen bonds in the crystal structures of 1-methyl-2-pyridin-4-yl-benzimidazole, haloaldoximes and their co-crystals.[2d] Desiraju and co-workers described the role of halogen bonds and hydrogen bonds in crystal engineering,[3a] and characterized their impact in crystals of mono- and polyfluorinated benzoic acids,[3b] dihalogenated phenols[3c] and 4-nitrobenzamide : diacid : 1,4-dihalogenated benzene co-crystals.[3d] Awwadi et al. studied the nature of halogen···halogen synthons and reported on N–H···X and X···X interactions in iodopyridinium tetrahalocuprate(II)[4a] and 2,5-dibromopyridinium halide salts.[4b] Bruce and co-workers investigated the formation of halogen and hydrogen bonds in the compounds obtained by the crystallization of 4-halotetrafluoro-phenols with 1,4-dithiane[5a] and cyclic secondary and tertiary amines.[5b] Ding et al. described the competing hydrogen bonding and halogen bonding in co-crystals formed from bi-functional donor molecules with two isomeric symmetric acceptors.[6] Katrusiak and co-workers discussed the effects of pressure on competition between C–H···X hydrogen bonds and X···X halogen bonds in crystals of halomethane compounds.[7] Santos-Contreras et al. examined the significance of non-covalent interactions (including halogen bonds) in 6-substituted 2-oxo-2H-chromene-3-carboxylic acids.[8] Finally, Woźniak and co-workers described the influence of a halogen substituent on the packing of halogen- and hydrogen-bonded crystals of boranthrenes.[9] In the context of investigations into the competition between halogen and hydrogen bonding in crystals, *ortho*- and *meta*- halobenzoic acids represent an interesting object of study. This follows directly from the fact that a search of the Cambridge Structure Database (CSD version 5.36, update November 2014)[10] shows that there are relatively few structures of organic co-crystals, salts or solvates formed from them (10, 21, 7 and 4 structures of compounds containing 2-fluorobenzoic acid,[10a] 2-chlorobenzoic acid,[10b] 2-bromobenzoic acid,[10c] and 2-iodobenzoic acid[10d] moieties respectively, and 11, 32, 8 and 14 structures of compounds containing 3-fluorobenzoic acid,[10e] 3-chlorobenzoic acid,[10f] 3-bromobenzoic acid,[10g] and 3-iodobenzoic acid[10h] moieties respectively – including the structures of the acids themselves).

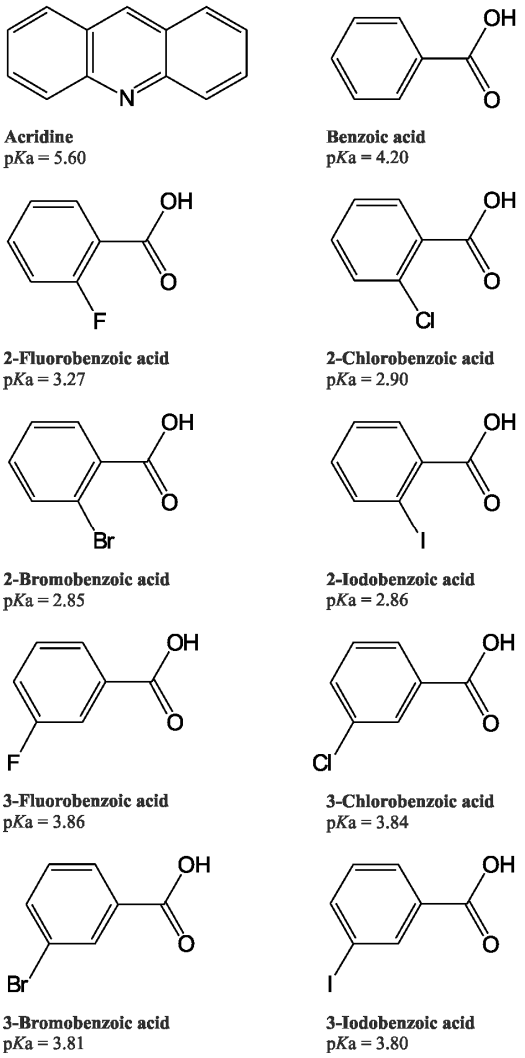

Scheme 1 Chemical structures of the co-crystal system components reported in this paper

In view of our interest in multicomponent systems formed by heterocyclic nitrogen bases and benzoic acids,[11] we examined the co-crystallization of complexes containing acridine and mono-substituted halobenzoic acids. Although crystallographic studies of proton transfer between acridine and acids (including benzoic acids) have been carried out,[12] structural investigations into the molecular complexes of acridine and *ortho*- and *meta*-halobenzoic acids have not been performed. Thus, in order to explain how the *ortho*- and *meta*- halogen substituent in the phenyl ring of the benzoic acid influences the formation and competition of C–H···X hydrogen-bonds and X···O halogen-bonds in the co-crystals formed from acridine and benzoic acids, we synthesized and structurally characterized the following compounds: acridine • benzoic acid (**1**), acridine • 2-fluorobenzoic acid (**2**), acridine • 2-chlorobenzoic acid (**3**), acridine • 2-bromobenzoic acid (**4**), acridine • 2-iodobenzoic acid (**5**), acridine • 3-fluorobenzoic acid (**6**), acridine • 3-chlorobenzoic acid (**7**), acridine • 3-bromobenzoic acid (**8**) and acridine • 3-iodobenzoic acid (**9**) co-crystals. The number, type and strength of hydrogen bonds, halogen bonds, and melting points of co-crystals **1**–**9** were compared.

Experimental Section

Synthesis and Characterization of Compounds 1–9

All the chemicals were purchased from Sigma Aldrich and used without further purification.

*Acridine • benzoic acid co-crystal (**1**)*

Acridine (0.050 g, 0.279 mmol) and benzoic acid (0.034 g, 0.278 mmol) were dissolved in 50 cm^3 of an ethanol/water mixture (10:1, v/v) and boiled for *ca.* 15 minutes. The clear solution was allowed to evaporate for a few days to give pale orange crystals of **1** (m.p. = 94.7 ºC).

*Acridine • 2-fluorobenzoic acid co-crystal (**2**)*

Acridine (0.050 g, 0.279 mmol) and 2-fluorobenzoic acid (0.039 g, 0.278 mmol) were dissolved in 50 cm^3 of an ethanol/water mixture (10:1, v/v) and boiled for *ca.* 15 minutes. The clear solution was allowed to evaporate for a few days to give orange crystals of **2** (m.p. = 99.0 ºC).

*Acridine • 2-chlorobenzoic acid co-crystal (**3**)*

Acridine (0.050 g, 0.279 mmol) and 2-chlorobenzoic acid (0.044 g, 0.281 mmol) were dissolved in 50 cm^3 of an ethanol/water mixture (10:1, v/v) and boiled for *ca.* 15 minutes. The clear solution was allowed to evaporate for a few days to give orange crystals of **3** (m.p. = 95.5 ºC).

*Acridine • 2-bromobenzoic acid co-crystal (**4**)*

Acridine (0.050 g, 0.279 mmol) and 2-bromobenzoic acid (0.056 g, 0.278 mmol) were dissolved in 50 cm^3 of an ethanol/water mixture (10:1, v/v) and boiled for *ca.* 15 minutes. The clear solution was allowed to evaporate for a few days to give pale brown crystals of **4** (m.p. = 93.5º C).

*Acridine • 2-iodobenzoic acid co-crystal (**5**)*

Acridine (0.050 g, 0.279 mmol) and 2-iodobenzoic acid (0.069 g, 0.278 mmol) were dissolved in 50 cm^3 of an ethanol/water mixture (10:1, v/v) and boiled for *ca.* 15 minutes. The clear solution was allowed to evaporate for a few days to give pale brown crystals of **5** (m.p. = 99.3 ºC).

*Acridine • 3-fluorobenzoic acid co-crystal (**6**)*

Acridine (0.050 g, 0.279 mmol) and 3-fluorobenzoic acid (0.039 g, 0.278 mmol) were dissolved in 50 cm^3 of an ethanol/water mixture (10:1, v/v) and boiled for *ca.* 15 minutes. The clear solution was allowed to evaporate for a few days to give pale orange crystals of **6** (m.p. = 122.9 ºC).

*Acridine • 3-chlorobenzoic acid co-crystal (**7**)*

Acridine (0.050 g, 0.279 mmol) and 3-chlorobenzoic acid (0.044 g, 0.281 mmol) were dissolved in 50 cm^3 of an ethanol/water mixture (10:1, v/v) and boiled for *ca.* 15 minutes. The clear solution was allowed to evaporate for a few days to give pale orange crystals of **7** (m.p. = 129.5 ºC).

*Acridine • 3-bromobenzoic acid co-crystal (**8**)*

Acridine (0.050 g, 0.279 mmol) and 3-bromobenzoic acid (0.056 g, 0.278 mmol) were dissolved in 50 cm^3 of an ethanol/water mixture (10:1, v/v) and boiled for *ca.* 15 minutes. The clear solution was allowed to evaporate for a few days to give orange crystals of **8** (m.p. = 137.3 ºC).

*Acridine • 3-iodobenzoic acid co-crystal (**9**)*

Acridine (0.050 g, 0.279 mmol) and 3-iodobenzoic acid (0.069 g, 0.278 mmol) were dissolved in 50 cm^3 of an ethanol/water mixture (10:1, v/v) and boiled for *ca.* 15 minutes. The clear solution was allowed to evaporate for a few days to give pale brown crystals of **7** (m.p. = 140.2 ºC).

Table 1 Crystal Data and Structure Refinement Parameters for compounds **1**–**9**.

Compound	**1**	**2**	**3**	**4**	**5**	**6**	**7**	**8**	**9**
Chemical formula	$(C_{13}H_9N)\bullet$ $(C_7H_6O_2)$	$(C_{13}H_9N)\bullet$ $(C_7H_5O_2F)$	$(C_{13}H_9N)\bullet$ $(C_7H_5O_2Cl)$	$(C_{13}H_9N)\bullet$ $(C_7H_5O_2Br)$	$(C_{13}H_9N)\bullet$ $(C_7H_5O_2I)$	$(C_{13}H_9N)\bullet$ $(C_7H_5O_2F)$	$(C_{13}H_9N)\bullet$ $(C_7H_5O_2Cl)$	$(C_{13}H_9N)\bullet$ $(C_7H_5O_2Br)$	$(C_{13}H_9N)\bullet$ $(C_7H_5O_2I)$
FW/g mol^{-1}	301.33	319.32	335.77	380.23	427.22	319.32	335.77	380.23	427.22
Crystal system	monoclinic	monoclinic	triclinic	triclinic	triclinic	triclinic	triclinic	triclinic	triclinic
Space group	$P2_1/n$	$P2_1/n$	P-1	P-1	P-1	P-1	P-1	P-1	P-1
a/Å	8.945(1)	6.990(1)	7.276(1)	7.355(1)	7.765(1)	6.889(2)	7.079(1)	7.095(1)	7.137(2)
b/Å	13.405(1)	23.197(4)	8.889(1)	8.938(1)	8.695(1)	8.789(2)	8.791(1)	8.753(2)	8.773(2)
c/Å	13.477(1)	9.882 (1)	13.217(1)	13.216(2)	13.303(1)	13.861(5)	13.803(1)	13.960(2)	14.291(1)
α/°	90	90	72.108(11)	72.73(1)	74.823(8)	74.83(3)	76.757(9)	77.328(15)	77.820(13)
β/°	105.006(3)	98.349(14)	82.067(7)	80.73(1)	86.113(9)	79.38(3)	83.524(8)	83.389(14)	81.659(13)
γ/°	90	90	89.098(8)	88.490(9)	82.446(9)	80.60(2)	78.472(9)	79.591(17)	79.743(17)
V/Å^3	1560.9(1)	1585.5(4)	805.4(2)	818.6(2)	858.8(2)	790.2(4)	817.2(2)	829.3(3)	855.2(3)
Z	4	4	2	2	2	2	2	2	2
T/K	295(2)	295(2)	295(2)	295(2)	295(2)	295(2)	295(2)	295(2)	295(2)
λ_{Mo}/Å	0.71073	0.71073	0.71073	0.71073	0.71073	0.71073	0.71073	0.71073	0.71073
ρ_{calc}/g cm^{-3}	1.282	1.338	1.385	1.543	1.652	1.342	1.365	1.523	1.659
$F(000)$	632.0	664	348	384	420	332	348	384	420
μ/mm^{-1}	0.083	0.095	0.249	2.522	1.876	0.095	0.245	2.490	1.883
2θ range/°	3.42–25.00	3.35–25.00	3.30–25.00	3.43–25.00	3.39–25.00	3.43–25.00	3.04–25.00	3.39–25.00	3.90–25.00
Completeness 2θ /%	99.6	99.5	99.8	99.7	99.5	99.5	98.6	99.5	99.4
Reflections collected	20140	10327	5615	5555	5757	4881	6365	5353	5398
Reflections unique	2738 [R_{int}=0.0392]	2783 [R_{int}=0.0351]	2828 [R_{int}=0.0192]	2879 [R_{int}=0.0419]	3008 [R_{int}=0.0665]	2766 [R_{int}=0.0224]	2842 [R_{int}=0.0165]	2921 [R_{int}=0.0392]	2992 [R_{int}=0.0226]
Data/restraints/ parameters	2738/1/212	2783/14/249	2828/8/250	2879/20/249	3008/1/220	2766/4/234	2842/1/222	2921/1/222	2992/1/222
Goodness-of-fit on F^2	1.065	1.094	1.013	1.037	1.060	1.039	1.055	0.986	1.042
Final R_1 value ($I > 2\sigma(I)$)	0.0411	0.0552	0.0448	0.0519	0.0514	0.0494	0.0400	0.0534	0.0365
Final wR_2 value ($I > 2\sigma(I)$)	0.0989	0.1301	0.1065	0.1288	0.1259	0.1235	0.1069	0.0914	0.0815
Final R_1 value (all data)	0.0468	0.0716	0.0722	0.0722	0.0596	0.0762	0.0498	0.0723	0.0463
Final wR_2 value (all data)	0.1023	0.1395	0.1262	0.1453	0.1354	0.1429	0.1116	0.1273	0.0867
CCDC number	1047946	1047947	1047948	1047949	1047950	1047951	1047952	1047953	1047945

X-ray measurements and refinements; determination of melting points

Good-quality single-crystal specimens of **1**–**9** were selected for the X-ray diffraction experiments at T = 295(2) K (Table 1). They were mounted with epoxy glue at the tip of glass capillaries. Diffraction data were collected on an Oxford Diffraction Gemini R ULTRA Ruby CCD diffractometer with Mo$K\alpha$ (λ = 0.71073 Å) radiation. In all cases, the lattice parameters were obtained by least-squares fit to the optimized setting angles of the reflections collected by means of *CrysAlis CCD*.[13a] Data were reduced using *CrysAlis RED* software[13a] and applying multi-scan absorption corrections (empirical absorption correction using spherical harmonics, implemented in the SCALE3 ABSPACK scaling algorithm). The structural resolution procedure was carried out using the *SHELX* package.[13b] The structures were solved with direct methods that carried out refinements by full-matrix least-squares on F^2 using the *SHELXL-97* program. The benzene rings in compounds **2**–**4**, i.e. 2-fluorobenzoic, 2-chlorobenzoic and 2-bromobenzoic acid molecules respectively, have orientation disorders with refined site-occupancy factors of the disordered parts 0.926 and 0.074 for compound **2**, 0.852 and 0.148 for compound **3** and 0.928 and 0.072 for compound **4** (in all cases, the disordered benzene rings were refined as rigid ideal hexagons with C–C = 1.39 Å and constrained with isotropic displacement parameters). In compound **6**, the fluorine atom and the C-atom bound to it from the 3-fluorobenzoic acid molecule have orientation disorders with refined site-occupancy factors of the disordered parts 0.870 and 0.130. All H-atoms bound to aromatic C-atoms were placed geometrically and refined using a riding model with C–H = 0.93 Å and $U_{iso}(H) = 1.2U_{eq}(C)$. All H-atoms bound to O-atoms were located on a Fourier difference map and refined restraints (DFIX command) where $U_{iso}(H)=1.5 U_{eq}(O)$. All interactions were found using the PLATON program.[13c] The ORTEPII,[13d] PLUTO-78[13e] and Mercury[13f] programs were used to prepare the molecular graphics. Melting points were determined on a Buchi 565 capillary apparatus and were uncorrected.

Results and discussion

*Crystal structure of acridine · benzoic acid co-crystal (**1**)*

The single crystal of compound **1** crystallized in the monoclinic $P2_1/n$ space group with one acridine molecule and one benzoic acid molecule in the asymmetric unit (Fig. 1a, Table 1). The C–O bond lengths [1.205(2)–1.317(2) Å] in the COOH group show that proton transfer has not occurred. The benzoic acid and acridine molecules are linked by O–H···N hydrogen bonds [*d*(O22···N10) = 2.668(2) Å and <(O22–H22···N10) = 173(2)°] to form heterodimers (Fig. 1a, Table 2). The neighbouring heterodimers, inverted *via* the crystallographic centre of inversion, are connected *via* C–H···O hydrogen bonds [*d*(C9···O23) = 3.353(2) Å and <(C9–H9···O23) = 147°] to form heterotetramers (Fig. 2a, Table 2). In these heterotetramers the acridine moieties interact *via* π–π interactions [with *centroid*···*centroid* distances *d*(Cg···Cg) from 3.640(1) to 3.840(1) Å and separation between the mean planes of the acridine skeleton 3.462(1) Å].

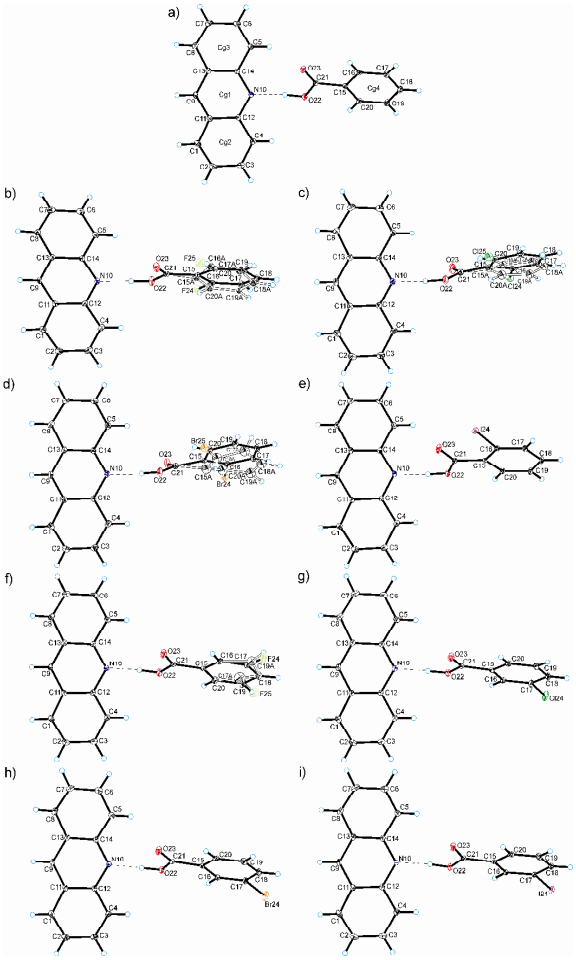

Figure 1 Molecular structures of compounds **1**–**9** showing the atom-labelling scheme. Displacement ellipsoids are drawn at the 25% probability level and H atoms are shown as small spheres of arbitrary radius. Cg1,Cg2, Cg3, Cg4 and Cg4A denote the ring centroids

In the crystal packing, the adjacent tetramers interact *via* weak C–H···O hydrogen bonds [*d*(C2···O22) = 3.615(2) Å and <(C2–H2···O22) = 150° and *d*(C6···O23) = 3.638(2) Å and <(C6–H6···O23) = 158°] between acridine and benzoic acid molecules and π–π interactions between the aromatic rings of benzoic acid [*d*(Cg···Cg) = 3.998(1) Å and separations 3.675(1) Å] to produce blocks along the *a*-axis. (Figs. 2b and 4a, Table 2). The neighbouring blocks are connected by C–H···π interactions between the benzoic acid molecules and the acridine skeleton [*d*(H16···Cg2) = 2.86Å and <(C16–H16···Cg2) = 148° and *d*(H20···Cg3) = 3.03 Å and <(C20–H20···Cg3) = 141°] to form a 3D framework structure (Fig. 2c, Table 2).

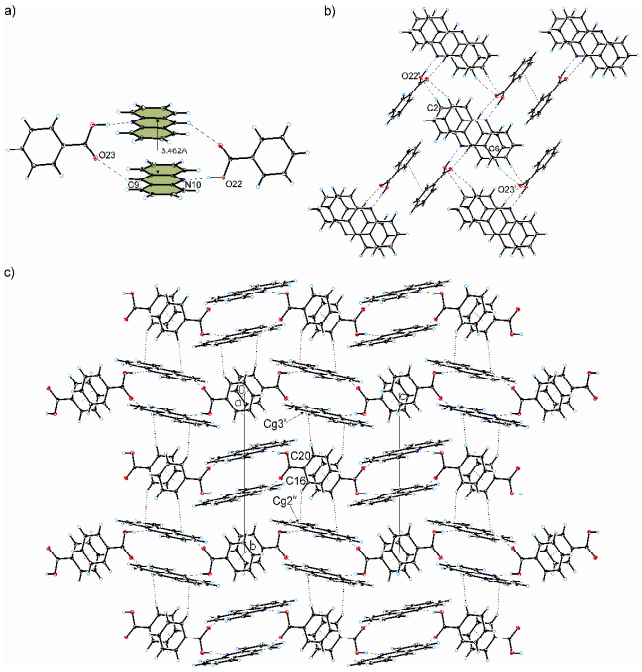

Figure 2 (a) Heterotetramers formed by acridine and benzoic acid in **1**. (b) Intermolecular interactions between heterotetramers in 1. (c) Crystal packing of **1** viewed along the *a*-axis (hydrogen bonds are represented by dashed lines and C–H···π and π–π interactions by dotted lines).

*Crystal structure of acridine·2-fluorobenzoic acid co-crystal (**2**)*

Single-crystal X-ray diffraction measurements show that compound **2** crystallized in the monoclinic $P2_1/n$ space group with one acridine and one 2-fluorobenzoic acid molecule in the asymmetric unit (Fig. 1b, Table 1). The C–O bond lengths [1.205(7)–1.276(7) Å] in the COOH group indicate that proton transfer has not occurred. The 2-fluorobenzoic acid molecule interacts with the acridine molecule *via* O–H···N hydrogen bonds [*d*(O22···N10) = 2.601(6) Å and <(O22–H22···N10) = 173(6)°] to form heterodimers (Fig. 1b, Table 2). The neighbouring inversion-related heterodimers are linked by C–H···O hydrogen bonds [*d*(C8···O23) = 3.556(7) Å and <(C9–H9···O23) = 141° and *d*(C9···O23) = 3.621(7) Å and <(C9–H9···O23) = 137°], forming heterotetramers (Fig. 3a, Table 2). The acridine moieties in these tetramers interact *via* π–π interactions [*d*(Cg···Cg)= 3.714(3)–3.755(3) Å and separation 3.474(3) Å]. The adjacent tetramers in the crystal packing interact *via* C–H···F hydrogen bonds [*d*(C20···F24) = 3.508(9) Å and <(C20–H20···F24) = 133° and *d*(C20A···F25) = 3.758(9) Å and <(C20A–H20A···F25) = 162°] and F···F halogen bonding interactions [*d*(F24···F25) = 2.807(9) Å] between 2-fluorobenzoic acid molecules, and *via* π–π interactions between the acridine skeleton [*d*(Cg···Cg)= 3.717(3)–3.859(3) Å and separation 3.513(3) Å] to produce columns along the *a*-axis (Figs. 4b and 5a, Table 2).

Table 2 Hydrogen-bonding geometry for compounds **1**–**5**.

Compound	D–H···A	*d*(D–H) (Å)	*d*(H···A) (Å)	*d*(D···A) (Å)	<D–H···A (°)
1	O22–H22···N10	0.98(2)	1.69(2)	2.668(2)	173(2)
	C9–H9···O23^{i}	0.93	2.54	3.353(2)	147
	C2–H2···O22^{ii}	0.93	2.78	3.615(2)	150
	C6–H6···O23^{iii}	0.93	2.76	3.638(2)	158
	C16–H16···Cg2^{iv}	0.93	2.86	3.684(2)	148
	C20–H20···Cg3^{v}	0.93	3.03	3.801(2)	141
Symmetry code: (i) 1–x, 1–y, –z; (ii) –1+x, y, z; (iii) 2–x, 1–y, –z; (iv) 3/2–x, ½+y, ½–z; (v) ½+x, ½–y, ½+z.					
2	O22–H22···N10	0.99(7)	1.62(7)	2.601(6)	173(6)
	C8–H8···O23^{i}	0.93	2.78	3.556(6)	141
	C9–H9···O23^{i}	0.93	2.86	3.621(6)	137
	C1–H1···Cg4^{ii}	0.93	3.18	4.104(6)	172
	C2–H2···F24^{iii}	0.93	2.56	3.382(9)	147
	C2–H2···F25^{iv}	0.93	2.66	3.164(9)	115
	C6–H6···Cg4^{v}	0.93	3.04	3.877(6)	151
	C17–H17···O23^{vi}	0.93	2.83	3.490 (6)	129
	C18–H18···F24^{vi}	0.93	2.81	3.324(9)	116
	C18A–H18A···F25^{vii}	0.93	2.54	3.283(9)	138
	C19–H19···O22^{vii}	0.93	3.05	3.670(6)	126
	C20–H20···F24^{viii}	0.93	2.81	3.508(9)	133
	C20A–H20A···F25^{ix}	0.93	2.87	3.758(9)	162
Symmetry code: (i) –x, 1–y, 1–z; (ii) 1–x, 1–y, 1–z; (iii) –1+x, –1+y, z; (iv) 1–x, –y, –z ; (v) x, y, 1+z; (vi) ½+x, ½–y, –½+z; (vii) –½+x, ½–y, –½+z; (viii) 1–x, –y, 2–z ; (ix) –1+x, y, z.					
3	O22–H22···N10	1.00(3)	1.61(3)	2.601(3)	171(3)
	C8–H8···O23^{i}	0.93	2.88	3.554(3)	130
	C9–H9···O23^{i}	0.93	2.65	3.409(3)	139
	C9–H9···Cl25^{ii}	0.93	3.07	3.781(6)	135
	C2–H2···Cg4^{iii}	0.93	3.04	3.845(3)	139
	C2–H2···Cl24^{iv}	0.93	3.14	3.654(3)	117
	C3–H3···O22^{iii}	0.93	2.70	3.570(3)	156
	C6–H6···Cl24^{ii}	0.93	2.96	3.815(3)	154
	C19–H19···Cl24^{v}	0.93	3.07	3.567(3)	115
Symmetry code: (i) 1–x, 2–y, 1–z; (ii) x, 1+y, z; (iii) 2–x, 1–y, 1–z;(iv) 1–x, 1–y, 1–z;(v) 1+x, y, z.					
4	O22–H22···N10	1.00(5)	1.62(5)	2.610(5)	171(5)
	C8–H8···O23^{i}	0.93	2.99	3.675(5)	131
	C9–H9···O23^{i}	0.93	2.67	3.389(5)	135
	C9–H9···Br25^{ii}	0.93	3.08	3.796(8)	135
	C2–H2···Cg4^{iii}	0.93	3.12	3.894(5)	142
	C2–H2···Br24^{iv}	0.93	3.12	3.598(5)	113
	C3–H3···O22^{iii}	0.93	2.67	3.555(5)	159
	C6–H6···Br24^{ii}	0.93	3.09	3.869(5)	154
	C19–H19···Br24^{v}	0.93	3.20	3.636(5)	111
Symmetry code: (i) 1–x, 2–y, 1–z; (ii) x, 1+y, z; (iii) 2–x, 1–y, 1–z;(iv) 1–x, 1–y, 1–z;(v) 1+x, y, z.					
5	O22–H22···N10	0.98(4)	1.65(4)	2.626(6)	176(6)
	C8–H8···O23^{i}	0.93	2.85	3.529(6)	131
	C9–H9···O23^{i}	0.93	2.42	3.197(6)	141
	C2–H2···I24^{ii}	0.93	3.41	4.226(6)	148
	C2–H2···O22^{iii}	0.93	2.97	3.663(6)	132
	C6–H6···O23^{iv}	0.93	2.76	3.625(6)	156
	C20–H20···I24^{v}	0.93	3.13	4.050(6)	172
Symmetry code: (i) 1–x, 1–y, 2–z; (ii) x+1, y+1, z; (iii) x, y–1, z; (iv) 1–x, 2–y, 2–z; (v) 1–x, y, z.					

The neighbouring columns interact *via* C–H···F hydrogen bonds [*d*(C2···F24) = 3.382(9) Å and <(C2–H2···F24) = 147° and *d*(C2···F25) = 3.164(9) Å and <(C2–H2···F25) = 115°] and C–H···π interactions between acridine and 2-fluorobenzoic acid molecules [*d*(H6···Cg4) = 3.04 Å and <(C6–H6···Cg4) = 151°] to produce blocks along the *c*-axis. (Figs. 4b and 5a, Table 2). The adjacent blocks are connected by weak C–H···π interactions between the acridine and 2-fluorobenzoic acid molecules [*d*(H1···Cg4) = 3.18 Å and <(C1–H1···Cg4) = 172°], C–H···O hydrogen bonds [*d*(C17···O23) = 3.490(6) Å and <(C17–H17···O23) = 129° and *d*(C19···O22) = 3.670(6) Å and <(C19–H19···O22) = 126°] and C–H···F hydrogen bonds [*d*(C18···F24) = 3.324(9) Å and <(C18–H18···F24) = 116° and *d*(C18A···F25) = 3.283(9) Å and <(C18A–H18A···F25) = 138°] between 2-fluorobenzoic acid molecules, forming a 3D structure (Fig. 5a, Table 2).

*Crystal structure of acridine·2-chlorobenzoic acid co-crystal (**3**)*

Single-crystal X-ray diffraction measurements show that compound **3** crystallized in the triclinic *P*-1 space group with one acridine and one 2-chlorobenzoic acid molecule in the asymmetric unit (Fig. 1c, Table 1). The C–O bond lengths [1.194(3)–1.284(3) Å] in the COOH group show that proton transfer has not occurred. The 2-chlorobenzoic acid molecule interacts with the acridine molecule *via* O–H···N hydrogen bonds [*d*(O22···N10) = 2.601(3) Å and <(O22–H22···N10) = 171(3)°] to form heterodimers (Fig. 1c, Table 2). The neighbouring inversion-related heterodimers are linked by C–H···O hydrogen bonds [*d*(C8···O23) = 3.554(3) Å and <(C8–H8···O23) = 130° and *d*(C9···O23) = 3.409(3) Å and <(C9–H9···O23) = 139°] to form heterotetramers (Fig. 3b, Table 2). The acridine moieties in

these tetramers interact *via* π–π interactions [*d*(Cg···Cg)= 3.637(2)–3.845(2) Å and separation 3.527(2) Å]. The adjacent tetramers in the crystal packing interact *via* C–H···Cl hydrogen bonds [*d*(C9···Cl25) = 3.781(6) Å and <(C9–H9···Cl25) = 135°] between acridine and 2-chlorobenzoic acid molecules, C–H···Cl hydrogen bonds [*d*(C19···Cl24) = 3.567(3) Å and <(C19–H19···Cl24) = 115°] between 2-chlorobenzoic acid molecules and π–π interactions between the acridine skeletons [*d*(Cg···Cg)= 3.892(2)–3.939(2) Å and separation 3.451(3) Å] to produce columns along the *a*-axis (Fig. 4c and 5b, Table 2). The neighbouring columns are linked by C–H···O hydrogen bonds [*d*(C3···O22) = 3.570(3) Å and <(C3–H3···O22) = 156°] and C–H···Cl hydrogen bonds [*d*(C2···Cl24) = 3.654(3) Å and <(C2–H2···Cl24) = 117° and *d*(C6···Cl24) = 3.815(3) Å and <(C6–H6···Cl24) = 154°] between acridine and benzoic acid molecules and C–H···π interactions between acridine and 2-chlorobenzoic acid molecules [*d*(H2···Cg4) = 3.04 Å and <(C2–H2···Cg4) = 139°] to produce blocks along the *b*-axis (Figs. 4c and 5b, Table 2). The adjacent blocks are connected by π–π interactions between the aromatic rings of 2-chlorobenzoic acid [*d*(Cg···Cg)= 3.818(2) Å and separation 3.615(2) Å] forming a 3D framework structure (Fig. 5b, Table 2).

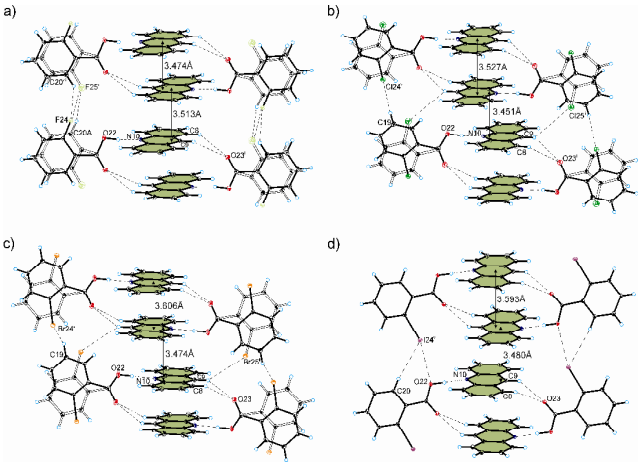

Figure 3 Heterotetramers formed by acridine and *ortho*-halobenzoic acids in compounds **2**–**5** (hydrogen bonds are represented by dashed lines).

*Crystal structure of acridine·2-bromobenzoic acid co-crystal (**4**)*

Single-crystal X-ray diffraction measurements show that compound **4** crystallized in the triclinic *P*-1 space group with one acridine and one 2-bromobenzoic acid molecule in the asymmetric unit (Fig. 1d, Table 1). The C–O bond lengths [1.202(3)–1.297(3) Å] in the COOH group indicate that proton transfer has not occurred. The 2-bromobenzoic acid molecule interacts with the acridine molecule *via* O–H···N hydrogen bonds [*d*(O22···N10) = 2.610(5) Å and <(O22–H22···N10) = 171(5)°] to form heterodimers (Fig. 1d, Table 2). The neighbouring inversion-related heterodimers are linked by C–H···O hydrogen bonds [*d*(C8···O23) = 3.675(5) Å and <(C8–H8···O23) = 131° and *d*(C9···O23) = 3.389(5) Å and <(C9–H9···O23) = 135°] to form heterotetramers (Fig. 3c, Table 2). The acridine moieties in these tetramers interact *via* π–π interactions [*d*(Cg···Cg)= 3.667(2)–3.978(2) Å and separation 3.606(2) Å]. In the crystal packing, the adjacent tetramers interact *via* C–H···Br hydrogen bonds [*d*(C9···Br25) = 3.796(8) Å and <(C9–H9···Br25) = 135°] between the acridine and 2-bromobenzoic acid molecules, C–H···Br hydrogen bonds [*d*(C19···Br24) = 3.636(5) Å and <(C19–H19···Br24) = 111°] between the 2-bromobenzoic acid molecules and π–π interactions between the acridine skeletons [*d*(Cg···Cg)= 3.927(2)–3.978(2) Å and separation 3.474(2) Å] to produce columns along the *a*-axis (Figs. 4d and 5c, Table 2). The neighbouring columns interact *via* C–H···O hydrogen bonds [*d*(C3···O22) = 3.555(5) Å and <(C3–H3···O22) = 159°] and C–H···Br hydrogen bonds [*d*(C2···Br24) = 3.598(5) Å and <(C2–H2···Br24) = 113° and *d*(C6···Br24) = 3.869(5) Å and <(C6–H6···Br24) = 154°] between the acridine and 2-bromobenzoic acid molecules and C–H···π interactions between the acridine and 2-bromobenzoic acid molecules [*d*(H2···Cg4) = 3.12 Å and <(C2–H2···Cg4) = 142°] to produce blocks along the *b*-axis (Figs. 4d and 5c, Table 2). The adjacent blocks are connected by π–π interactions between the aromatic rings of 2-bromobenzoic acid [*d*(Cg···Cg)= 3.798(2) Å and separation 3.589(2) Å] forming a 3D structure Fig. 5c, Table 2).

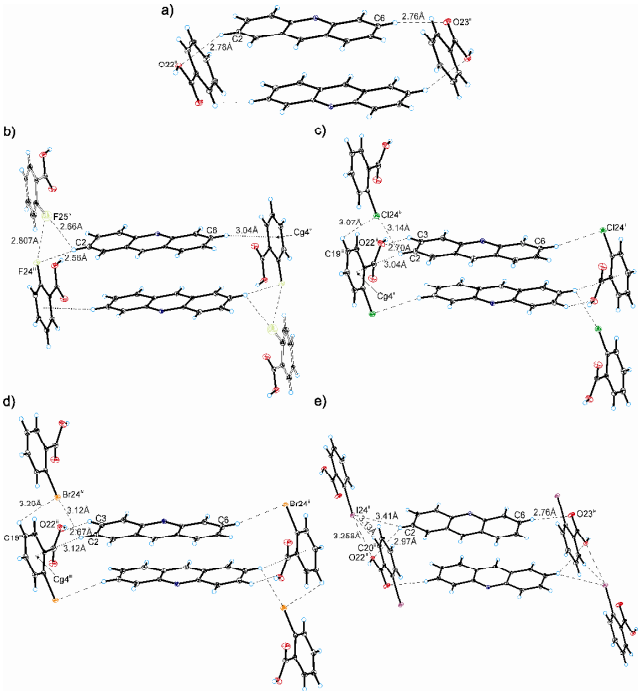

Figure 4 Connectivity of the neighbouring columns in the crystal packing of compounds **1**–**5** (hydrogen bonds are represented by dashed lines and C–H···π interactions by dotted lines).

*Crystal structure of acridine·2-iodobenzoic acid co-crystal (**5**)*

Single-crystal X-ray diffraction measurements show that compound **5** crystallized in the triclinic *P*-1 space group with one acridine and one 2-iodobenzoic acid molecule in the asymmetric unit (Fig. 1e, Table 1). The C–O bond lengths [1.199(6)–1.288(6) Å] in the COOH group show that proton transfer has not occurred. The 2-iodobenzoic acid molecule interacts with the acridine molecule *via* O–H···N hydrogen bonds [*d*(O22···N10) = 2.626(6) Å and <(O22–H22···N10) = 176(6)°] to form heterodimers (Fig. 1e, Table 2). The neighbouring inversion-related heterodimers are linked by C–H···O hydrogen bonds [*d*(C8···O23) = 3.529(6) Å and <(C8–H8···O23) = 131° and *d*(C9···O23) = 3.197(6) Å and <(C9–H9···O23) = 141°], to form heterotetramers (Fig. 3d, Table 2).

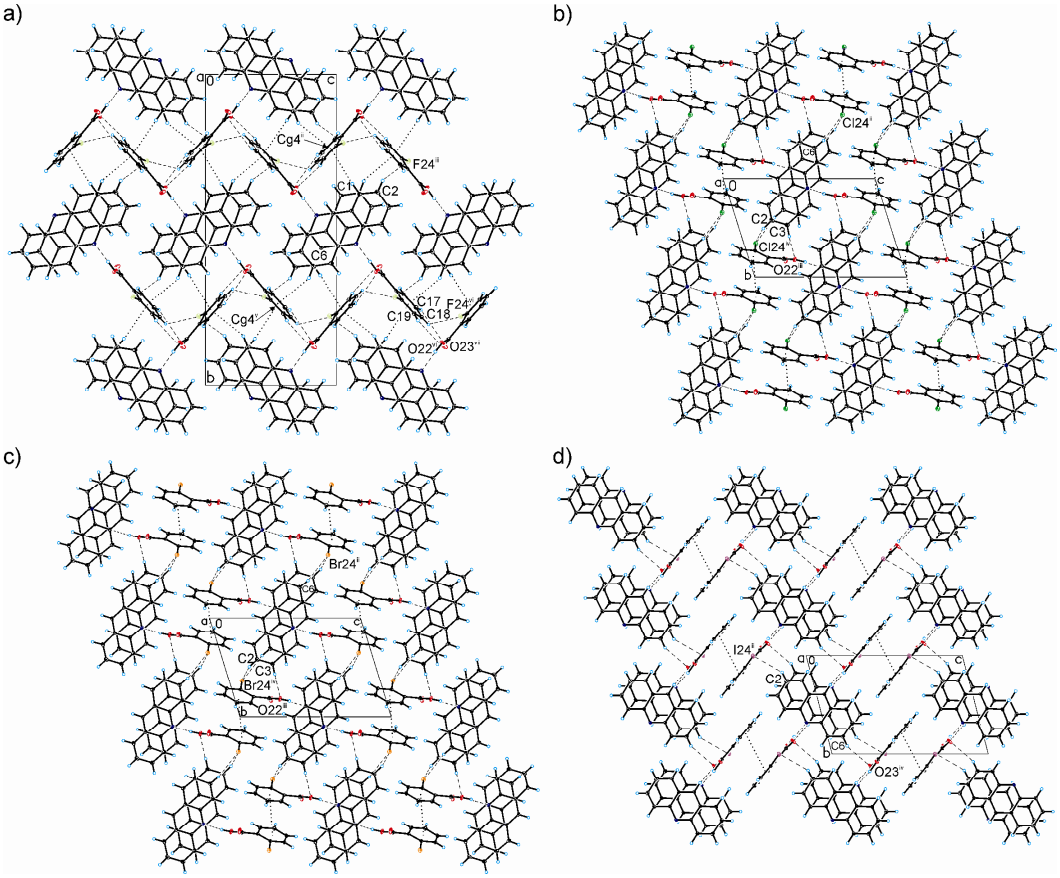

Figure 5 Crystal packing of compounds **2**–**5** viewed along the *a*-axis (hydrogen bonds are represented by dashed lines and C–H···π and π–π interactions by dotted lines).

The acridine moieties in these tetramers interact *via* π–π interactions [*d*(Cg···Cg)= 3.724(3)–4.126(3) Å and separation 3.593(3) Å]. In the crystal packing, the adjacent tetramers interact *via* C–H···I hydrogen bonds [*d*(C20···I24) = 4.050(6) Å and <(C20–H20···I24) = 172°] and I···O halogen bonds [*d*(I24···O22) = 3.258(4) Å] between the 2-iodobenzoic acid molecules, and π–π interactions between the acridine skeletons [*d*(Cg···Cg)= 3.760(3)–3.844(3) Å and separation 3.480(3) Å] to produce columns along the *a*-axis (Fig. 4e and 5d, Table 2). The neighbouring columns interact *via* C–H···O hydrogen bonds [*d*(C2···O22) = 3.663(6) Å and <(C2–H2···O22) = 132°] and *d*(C6···O23) = 3.625(6) Å and <(C6–H6···O22) = 156°] and C–H···I hydrogen bonds [*d*(C2···I24) = 4.226(6) Å and <(C2–H2···I24) = 148°] between the acridine and 2-iodobenzoic acid molecules to produce blocks along the *b*-axis (Figs. 4e and 5d, Table 2). The adjacent blocks are connected by π–π interactions between the aromatic rings of 2-iodobenzoic acid [*d*(Cg···Cg)= 3.896(3) Å and separation 3.561(3) Å] forming a 3D structure (Fig. 5d, Table 2).

*Crystal structure of acridine·3-fluorobenzoic acid co-crystal (**6**)*

Single-crystal X-ray diffraction measurements show that compound **6** crystallized in the triclinic *P*-1 space group with one acridine and one 3-fluorobenzoic acid molecule in the asymmetric unit (Fig. 1f, Table 1). The C–O bond lengths [1.208(2)–1.291(2) Å] in the COOH group indicate that proton transfer has not occurred. The 3-fluorobenzoic acid molecule interacts with the acridine molecule *via* O–H···N hydrogen bonds [*d*(O22···N10) = 2.601(2) Å and <(O22–H22···N10) = 175(2)°] to form heterodimers (Fig. 1f, Table 3). The neighbouring inversion-related heterodimers are linked by C–H···O hydrogen bonds [*d*(C9···O23) = 3.366(3) Å and <(C9–H9···O23) = 145°] to form heterotetramers (Fig. 6a, Table 3). The acridine moieties in these tetramers interact *via* π–π interactions [*d*(Cg···Cg)= 3.643(2)–3.757(2) Å and separation 3.449(2) Å]. In the crystal packing, the adjacent tetramers interact *via* π–π interactions between the acridine skeletons [*d*(Cg···Cg)= 3.663(2)–3.774(2) Å and separation 3.437(2) Å] to produce columns along the *a*-axis (Figs. 6a and 8a). The neighbouring columns interact *via* C–H···O hydrogen bonds [*d*(C2···O22) = 3.610(3) Å and <(C2–H2···O22) = 143°, and *d*(C6···O23) = 3.614(3) Å and <(C6–H6···O23) = 151°] and C–H···F hydrogen bonds [*d*(C3···F24) = 3.464(3) Å and <(C3–H3···F24) = 140°] between the acridine and 3-fluorobenzoic acid molecules to produce blocks along the *b*-axis (Figs. 7a and 8a, Table 3). The adjacent blocks are connected by C–H···F hydrogen bonds [*d*(C4···F24) = 3.342(3) Å and <(C4–H4···F24) = 138°, *d*(C4···F25) = 3.442(9) Å and <(C4–H4···F25) = 127° and *d*(C8···F25) = 3.841(9) Å and <(C8–H8···F25) = 107°], F···O halogen bonds [*d*(F25···O22) = 3.302(9) Å] and π–π interactions between the aromatic rings of 3-fluorobenzoic acid [*d*(Cg···Cg)= 3.938(2) Å and separation 3.709(2) Å] forming a 3D framework structure (Fig. 8a, Table 3).

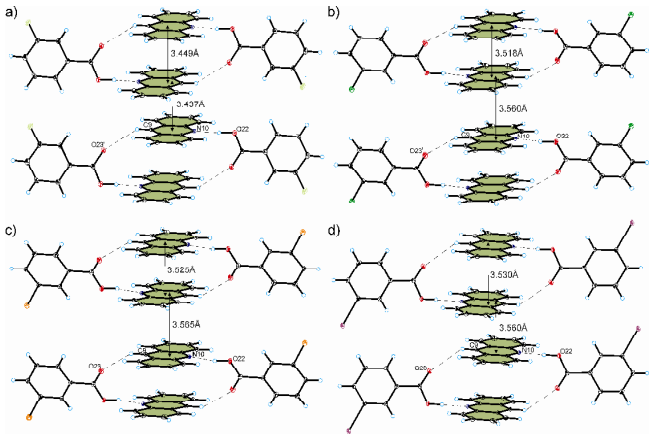

Figure 6 Heterotetramers formed by acridine and *meta*-halobenzoic acids in compounds **6**–**9** (hydrogen bonds are represented by dashed lines).

*Crystal structure of acridine·3-chlorobenzoic acid co-crystal (**7**)*

Single-crystal X-ray diffraction measurements show that compound **7** crystallized in the triclinic *P*-1 space group with one acridine and one 3-chlorobenzoic acid molecule in the asymmetric unit (Fig. 1g, Table 1). The C–O bond lengths [1.204(2)–1.302(2) Å] in the COOH group indicate that proton transfer has not occurred. The 3-chlorobenzoic acid molecule interacts with acridine *via* O–H···N hydrogen bonds [*d*(O22···N10) = 2.601(2) Å and <(O22–H22···N10) = 174(2)°] to form heterodimers (Fig. 1g, Table 3). The neighbouring inversion-related heterodimers are linked by C–H···O hydrogen bonds [*d*(C9···O23) = 3.383(3) Å and <(C9–H9···O23) = 144°] to form heterotetramers (Fig. 6b, Table 3). The acridine moieties in these tetramers interact *via* π–π interactions [*d*(Cg···Cg)= 3.665(1)–3.853(1) Å and separation 3.518(1) Å]. In the crystal packing, the adjacent tetramers interact *via* π–π interactions between the acridine skeletons [*d*(Cg···Cg)= 3.706(1)–3.899(1) Å and separation 3.560(1) Å] to produce columns along the *a*-axis (Figs. 6b and 8b). The neighbouring columns interact *via* C–H···O hydrogen bonds [*d*(C2···O22) = 3.604(3) Å and <(C2–H2···O22) = 140° and *d*(C6···O23) = 3.558(3) Å and <(C6–H6···O23) = 154°] between the acridine and 3-chlorobenzoic acid molecules to produce blocks along the *b*-axis (Figs. 7b and 8b, Table 3). The adjacent blocks are connected by C–H···Cl hydrogen bonds [*d*(C4···Cl24) = 3.841(3) Å and <(C4–H4···Cl24) = 130°, *d*(C8···Cl24) = 3.850(3) Å, <(C8–H8···Cl24) = 147° and *d*(C16···Cl24) = 3.937(3) Å and <(C16–H16···Cl24) = 162°], Cl···O halogen bonds [*d*(Cl24···O22) = 3.399(3) Å] and π–π interactions between the aromatic rings of 3-chlorobenzoic acid [*d*(Cg···Cg)= 3.859(1) Å and separation 3.603(1) Å] forming a 3D framework structure (Fig. 8b, Table 3).

*Crystal structure of acridine·3-bromobenzoic acid co-crystal (**8**)*

Single-crystal X-ray diffraction measurements show that compound **8** crystallized in the triclinic *P*-1 space group with one acridine and one 3-bromobenzoic acid molecule in the asymmetric unit (Fig. 1h, Table 1). The C–O bond lengths [1.206(4)–1.311(4) Å] in the COOH group indicate that proton transfer has not occurred. The 3-bromobenzoic acid molecule interacts with the acridine molecule *via* O–H···N hydrogen bonds [*d*(O22···N10) = 2.596(4) Å and <(O22–H22···N10) = 171(4)°] to form heterodimers (Fig. 1h, Table 3). The neighbouring inversion-related heterodimers are linked by C–H···O hydrogen bonds [*d*(C9···O23) = 3.385(5) Å and <(C9–H9···O23) = 143°] to form heterotetramers (Fig. 6c, Table 3). The acridine moieties in these tetramers interact *via* π–π interactions [*d*(Cg···Cg)= 3.645(2)–3.876(2) Å and separation 3.525(2) Å]. In the crystal packing, the adjacent tetramers interact *via* π–π interactions between the acridine skeletons [*d*(Cg···Cg)= 3.725(2)–3.976(2) Å and separation 3.565(2) Å] to produce columns along the *a*-axis (Figs. 6c and 8c). The neighbouring columns interact *via* C–H···O hydrogen bonds [*d*(C2···O22) = 3.626(5) Å and <(C2–H2···O22) = 139° and *d*(C6···O23) = 3.552(5) Å and <(C6–H6···O23) = 152°] between the acridine and 3-bromobenzoic acid molecules to produce blocks along the *b*-axis (Figs. 7c and 8c, Table 3). The adjacent blocks are connected by C–H···Br hydrogen bonds [*d*(C4···Br24) = 3.885(5) Å and <(C4–H4···Br24) = 127°, *d*(C8···Br24) = 3.947(5) Å and <(C8–H8···Br24) = 150° and *d*(C16··· Br24) = 4.005(5) Å and <(C16–H16···Br24) = 167°], Br···O halogen bonds [*d* (Br24···O22) = 3.415(4) Å] and π–π interactions between the aromatic rings of 3-bromobenzoic acid [*d*(Cg···Cg)= 3.855(2) Å and separation 3.583(2) Å] forming a 3D structure (Fig. 8c, Table 3).

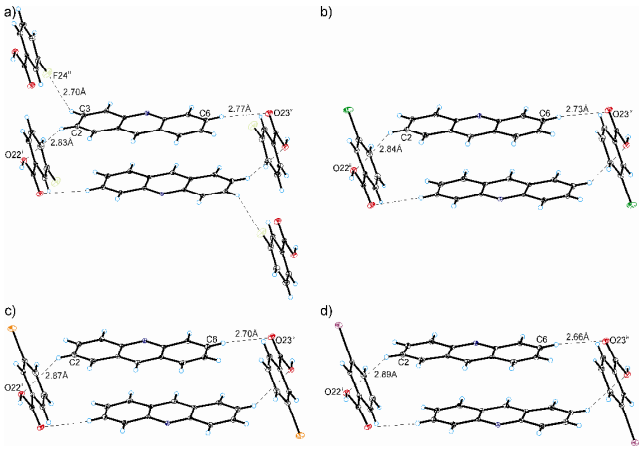

Figure 7 Connectivity of the neighbouring columns in the crystal packing of compounds **6**–**9** (hydrogen bonds are represented by dashed lines).

*Crystal structure of acridine·3-iodobenzoic acid co-crystal (**9**)*

Single-crystal X-ray diffraction measurements show that compound **9** crystallized in the triclinic *P*-1 space group with one acridine and one 3-iodobenzoic acid molecule in the asymmetric unit (Fig. 1i, Table 1). The C–O bond lengths [1.200(4)–1.313(4) Å] in the COOH group show that proton transfer has not occurred. The 3-iodobenzoic acid molecule interacts with the acridine molecule *via* O–H···N hydrogen bonds [*d*(O22···N10) = 2.611(4) Å and <(O22–H22···N10) = 173(4)°] to form heterodimers (Fig. 1i, Table 3). The neighbouring inversion-related heterodimers are linked by C–H···O hydrogen bonds [*d*(C9···O23) = 3.381(5) Å and <(C9–H9···O23) = 142°] to form heterotetramers (Fig. 6d, Table 3). The acridine moieties in these tetramers interact *via* π–π interactions [*d*(Cg···Cg)= 3.637(2)–3.866(2) Å and separation 3.530(2) Å]. In the crystal packing, the adjacent tetramers interact *via* π–π interactions between the acridine skeletons [*d*(Cg···Cg)= 3.734(2)–4.205(2) Å and separation 3.560(2) Å] to produce columns along the *a*-axis (Figs. 6d and 8d).

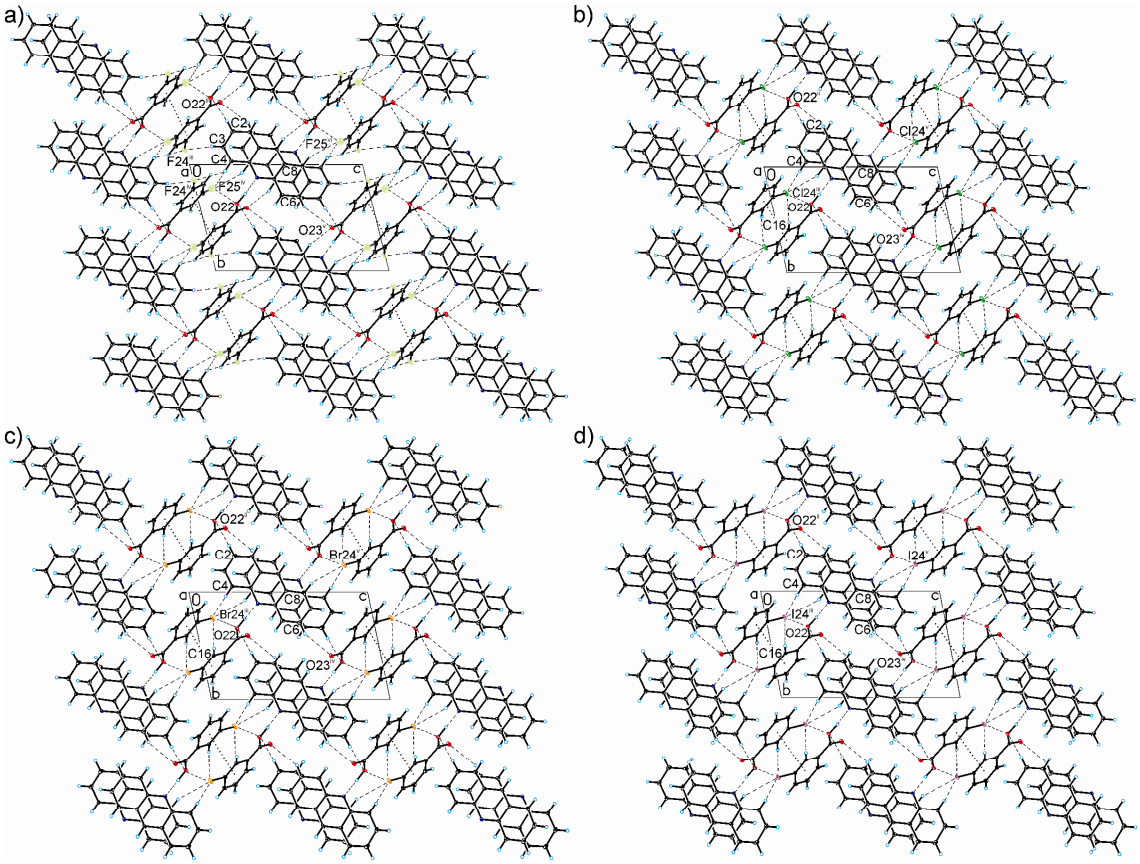

Figure 8 Crystal packing of compounds **6**–**9** viewed along the *a*-axis (hydrogen bonds and halogen bonds are represented by dashed lines and π–π interactions by dotted lines).

The neighbouring columns interact *via* C–H···O hydrogen bonds [*d*(C2···O22) = 3.646(5) Å and <(C2–H2···O22) = 140° and *d*(C6···O23) = 3.513(5) Å and <(C6–H6···O23) = 152°] between the acridine and 3-iodobenzoic acid molecules to produce blocks along the *b*-axis (Figs. 7d and 8d, Table 3). The adjacent blocks are connected by C–H···I hydrogen bonds [*d*(C4···I24) = 4.026(5) Å and <(C4–H4···I24) = 122°, *d*(C8···I24) = 4.113(5) Å and <(C8–H8···I24) = 153° and *d*(C16··· I24) = 4.105(5) Å and <(C16–H16··· I24) = 173°], I···O halogen bonds [d(I24···O22) = 3.468(4) Å] and π–π interactions between the aromatic rings of 3-iodobenzoic acid [*d*(Cg···Cg)= 3.940(2) Å and separation 3.612(2) Å] forming a 3D framework structure (Fig. 8d, Table 3).

*Supramolecular features of co-crystals **1**–**9***

As mentioned above, proton transfer does not occur and co-crystals are formed in all the compounds **1**–**9**. Investigation of co-crystal formation in terms of ΔpK_a values (Table 4)[14] demonstrates that these values are higher (2.33–2.74) for the co-crystals formed from acridine and *ortho*-halobenzoic acids than for co-crystals **6**–**9** (1.74–1.80). The value of ΔpK_a is the highest for compound **1** (1.40). Similar values were obtained for the recently described co-crystals of acridine and carboxylic acids[12f]. Confirmation that proton transfer does not take place emerges from the examination of certain geometric parameters characterizing acridine and halobenzoic acid molecules (Table 4). This is observed as the difference between the C–O and C=O bond lengths in the carboxyl group in a halobenzoic acid (ΔD)[15] ranging from 0.08 to 0.11 Å. This correlates with ΔpK_a only for co-crystals of acridine and *meta*-halobenzoic acids. In turn, the C12–N10–C14 valence angles are similar in all cases and range from 119 to120°, which indicates co-crystal formation. Analysis of CSD shows that this angle respectively ranges from 119 to 120° and from 123 to 124° in the co-crystal and salts formed from acridine and carboxylic acids. In all compounds **1**–**9**, the acridine skeleton is nearly planar. However, for compounds **2**–**4** the right-hand half of the acridine skeleton makes an angle of 1.6, 1.6 and 1.8° with the left-hand half in co-crystals of **2**, **3** and **4** respectively. This is probably because the benzene ring in halobenzoic acids has orientation disorders in these compounds. In the co-crystals of the other compounds this angle is no greater than 0.9°. Investigation of the O–H···N hydrogen bond in heterodimers indicates that the O22···N10 distance in co-crystal of **1** is longer (2.67 Å) than that in compounds **2**–**9** (2.60–2.62 Å). However, the C9···O23 distance in the C–H···O hydrogen bond between heterodimers is shorter (3.35 Å) for **1** than in most of the other compounds (3.38 to 3.41 Å). The C···O distance is the shortest in compound **5** (3.20 Å) and the longest in compound **2** (3.62 Å). This is because the heterodimers are linked by C9–H9···O22 hydrogen bonds in all the co-crystals analysed here, although these interactions are accompanied by C8–H8···O22 hydrogen bonds in co-crystals **2**–**5**. The formation of the C–H···O hydrogen bonds between heterodimers is directly associated with the mutual arrangement of the carboxyl group and acridine skeleton in dimers.

Table 3 Hydrogen-bonding geometry for compounds **6–9**.

Compound	D–H···A	*d*(D–H) (Å)	*d*(H···A) (Å)	*d*(D···A) (Å)	<D–H···A (°)
6	O22–H22···N10	0.99(2)	1.61(2)	2.601(2)	175(2)
	C9–H9···O23^{i}	0.93	2.56	3.366(3)	145
	C2–H2···O22^{ii}	0.93	2.83	3.610(3)	143
	C3–H3···F24^{iii}	0.93	2.70	3.464(3)	140
	C4–H4···F24^{iv}	0.93	2.60	3.342(3)	138
	C4–H4···F25^{iv}	0.93	2.80	3.442(9)	127
	C6–H6···O23^{v}	0.93	2.77	3.614(3)	151
	C8–H8···F25^{vi}	0.93	3.04	3.841(9)	107
Symmetry code: (i) 1–x, 2–y, 1–z; (ii) x, 1+y, z; (iii) –1+x, 1+y, z; (iv) 1–x, 1–y, 2–z; (v) 1–x, 1–y, 1–z; (vi) x, 1+y, –1+z.					
7	O22–H22···N10	0.99(2)	1.61(2)	2.601(2)	174(2)
	C9–H9···O23^{i}	0.93	2.58	3.383(3)	144
	C2–H2···O22^{ii}	0.93	2.84	3.604(3)	140
	C4–H4···Cl24^{iii}	0.93	3.17	3.841(3)	130
	C6–H6···O23^{iv}	0.93	2.73	3.558(3)	154
	C8–H8···Cl24^{v}	0.93	3.03	3.850(3)	147
	C16–H16···Cl24^{iii}	0.93	3.04	3.937(3)	162
Symmetry code: (i) 1–x, 2–y, –z; (ii) x, 1+y, z; (iii) –x, 1–y, 1–z; (iv) x, 1+y, –1+z; (v) –x, 1–y, 1–z.					
8	O22–H22···N10	0.98(3)	1.62(3)	2.596(4)	171(4)
	C9–H9···O23^{i}	0.93	2.59	3.385(5)	143
	C2–H2···O22^{ii}	0.93	2.87	3.626(5)	139
	C4–H4···Br24^{iii}	0.93	3.25	3.885(5)	127
	C6–H6···O23^{iv}	0.93	2.70	3.552(5)	152
	C8–H8···Br24^{v}	0.93	3.11	3.947(5)	150
	C16–H16···Br24^{iii}	0.93	3.09	4.005(5)	167
Symmetry code: (i) 2–x, 2–y, 1–z; (ii) x, 1+y, z; (iii) 1–x, 1–y, 2–z; (iv) 2–x, 1–y, 1+z; (v) x, 1+y, –1+z.					
9	O22–H22···N10	0.98(3)	1.64(3)	2.611(4)	173(4)
	C9–H9···O23^{i}	0.93	2.60	3.381(5)	142
	C2–H2···O22^{ii}	0.93	2.89	3.646(5)	140
	C4–H4···I24^{iii}	0.93	3.46	4.026(5)	122
	C6–H6···O23^{iv}	0.93	2.66	3.513(5)	152
	C8–H8···I24^{v}	0.93	3.26	4.113(5)	153
	C16–H16···I24^{iii}	0.93	3.18	4.105(5)	173
Symmetry code: (i) 2–x, 2–y, 1–z; (ii) x, 1+y, z; (iii) 1–x, 1–y, 2–z; (iv) 2–x, 1–y, 1+z; (v) x, 1+y, –1+z.					

The angle between the mean planes of the carboxyl group and the acridine skeleton ranges from 60.9 to 68.6° in compounds **1**, **5–9**, and is 83.0, 76.8 and 76.0° in compounds **2**, **3** and **4** respectively. Examination of the π–π interactions between the heterodimers in the title compounds confirms that the distance between the mean planes of adjacent acridine skeletons increases with increasing size of the substituent in the range of 3.46–3.60 Å and 3.45–3.53 Å for co-crystals **1–5**, and **6–9** respectively. An analysis of the π–π interactions between the acridine moieties in the crystal packing of seven known polymorphs of acridine (defined by Mei and Wolf[12f] as I-VII) indicates that π–stacked homodimers are formed in the polymorphic forms II, III and VII. In these homodimers, the distance between the mean planes of neighbouring acridine skeletons is in the range of 3.42 to 3.49 Å, which indicates that the presence of the halobenzoic acid influences on the arrangement of acridine molecules in the crystal packings of title compounds. Studies of interactions between neighbouring tetramers indicate that five types of interactions – π–π, C–H···O, C–H···X, X···X and X···O – can be observed. In compound **1**, π–stacking interactions between acridine moieties are absent, and the adjacent tetramers are linked by the C2–H2···O22 and C6–H6···O23 hydrogen bonds between the acridine and benzoic acid molecules, and π–π interactions between the aromatic rings of the benzoic acid molecules produce blocks. In compounds **2–9**, the neighbouring tetramers interact *via* π–π interactions, with the distance between the mean planes of neighbouring acridine skeletons ranging from 3.43 to 3.56 Å, as a result of which π-stacked columns of acridine moieties are formed. For comparison, in the case of the crystal structures of of acridine polymorphs the π–stacked columns of acridine moieties are absent, and adjacent tetramers are linked by C–H···π interactions. C–H···X hydrogen bonds between adjacent tetramers are only observed in the co-crystals formed from acridine and *ortho*-halobenzoic acids. However, these hydrogen bonds may occur between halobenzoic acids or acridine and halobenzoic acid molecules, depending on the mutual arrangement of the carboxyl group and benzene ring in the benzoic acid molecule. The angle between the mean planes of the carboxyl group and the benzene ring ranges from 2.6 to 29.6° and are ordered **1**<**2**<**5**<**3**<**4** in compounds **1–5**, and from 2.6 to 6.1° in the order **6**<**7**<**8**<**9** in compounds **6–9**. In compounds **2** and **5** this angle is 2.9° and 6.3° respectively, and in these cases a C20–H20···X hydrogen bond is present, whereas in the co-crystals of **3** and **4** this angle is 27.7° and 29.6° respectively, and a C19–H19···X hydrogen bond is present in their crystals. Additionally, in the co-crystals of acridine • 2-chloro- and 2-bromobenzoic acids, disordered chlorine and bromine atoms are involved only in one C9–H9···X hydrogen bond between acridine and halobenzoic acid molecules, whereas in the co-crystals of acridine • 2-fluorobenzoic acid a disordered fluorine atom participates in the F24···F25 halogen bond, C20A–H20A···F25A hydrogen bond between the tetramers and other C–H···F interactions. The I24···O22 halogen bond between adjacent tetramers occurs only in the co-crystals of acridine and 2-iodobenzoic acid.

Table 4 Selected geometric parameters characterizing the acridine and benzoic acid molecules and ΔpK_a in the title compounds.

Compound	*d*(C–O) / Å	*d*(C=O) / Å	ΔD[a] / Å	pK_a of acid[14]	ΔpK_a[b]	<(C12–N10···C14) /°	A[c] /°	*d*(O22···N10) / Å	*d*(C9···O23) / Å	B[d] /°	C[e] /°
1	1.317	1.205	0.112	4.20	1.40	119.1	0.7	2.67	3.35	64.5	2.6
2	1.276	1.205	0.071	3.27	2.33	120.4	1.6	2.60	3.62	83.0	2.9
3	1.284	1.194	0.090	2.90	2.70	119.8	1.6	2.60	3.41	76.8	27.7
4	1.297	1.202	0.095	2.85	2.75	119.4	1.8	2.61	3.39	76.0	29.6
5	1.288	1.199	0.089	2.86	2.74	119.3	0.8	2.62	3.20	63.1	6.3
6	1.291	1.208	0.083	3.86	1.74	119.8	0.1	2.60	3.37	68.6	2.6
7	1.302	1.204	0.098	3.84	1.76	120.0	0.7	2.60	3.38	68.0	2.9
8	1.311	1.206	0.105	3.81	1.79	119.5	0.5	2.60	3.38	64.1	2.9
9	1.313	1.200	0.113	3.80	1.80	119.5	0.9	2.61	3.38	60.9	6.1

[a] ΔD= *d*(C–O)– *d*(C=O); [b] $\Delta pK_a = pK_{a(base)} - pK_{a(acid)}$; p$K_a$ of acridine is 5.60; [c] angle between the mean planes of the right-hand and left-hand halves of the acridine skeleton; [d] angle between mean planes of carboxyl group and acridine skeleton; [e] angle between mean planes of carboxyl group and benzene ring.

Such differences are also observed in the connectivity of adjacent columns, which form blocks in the crystal packing of **2**–**9**. In the co-crystals formed from acridine and *ortho*-halobenzoic acids, the neighbouring columns are linked by C–H···O, C–H···π or C–H···X hydrogen bonds. In compound **2**, C2–H2···F24 and C2–H2···F25 hydrogen bonds are present as well as C6–H6···π interactions. In compounds **3** and **4**, all the above-mentioned interactions, such as C2–H2···π, C2–H2···X, C3–H3···O22, and C6–H6···X hydrogen bonds, are observed, but C–H···X are weaker than those found in **2**. In turn, the C2–H2···O22 and C6–H6···O23 hydrogen bonds and the C2–H2···I24 hydrogen bond are present in **5**. In all the co-crystals formed from acridine and *meta*-halobenzoic acids, the neighbouring columns are linked by C2–H2···O22 and C6–H6···O23 hydrogen bonds. Additionally, the C3–H3···F24 hydrogen bond is present in the crystal of **6**. Finally, analysis of interactions between adjacent blocks shows that C16–H16···π and C20–H20···π interactions occur in the crystal of **1**. In the crystal of **2**, C1–H1···π interactions as well as C–H···O hydrogen bonds (C17–H17···O23 and C19–H19···O22) and C–H···F hydrogen bonds (C18–H18···F24 and C18A–H18A···F25) are observed. In compounds **3**–**5**, the adjacent blocks are linked only by π–π interactions between aromatic rings of halobenzoic acid molecules. It is worth noting that this interaction does not occur in the co-crystal of acridine and 2-fluorobenzoic acid. The π–π interactions between the aromatic rings of halobenzoic acid molecules also occur in compounds **6**–**9**, however, these interactions are accompanied by C4–H4···X, C8–H8···X, C16–H16···X hydrogen bonds and a X···O22 halogen bonds.

Melting points and competition between C–H···X hydrogen bonds and X···X halogen bonds in the title compounds

Since the number, type and strength of intermolecular interactions occurring in the crystals of the title compounds have been compared with their melting points in the literature,[16] we decided to explain how the presence of hydrogen bonds and halogen bonds affects the melting points of these compounds. Analysis of these melting points shows that the co-crystal formed by acridine and benzoic and *ortho*-halobenzoic acids melts at a lower temperature than the separate components of the co-crystals: acridine (m.p. = 100.8 °C) and the corresponding benzoic acids (Table 5). The melting points are 94.7, 99.0, 95.5, 93.5, 99.3°C for compounds **1**–**5**, respectively, and are ordered as follows: **4**<**1**<**3**<**2**<**5**. Another tendency is observed for co-crystals formed from acridine and *meta*-halobenzoic acids: compounds **6**–**9** have higher melting points than acridine, but lower ones than the corresponding benzoic acids (Table 5). The melting points are 122.9, 129.5, 137.3 and 140.2°C for compounds **6**–**9**, respectively, and are ordered thus: **6**<**7**<**8**<**9**. This indicates that the melting points of compounds **6**–**9** rise with decreasing electronegativities of the halogen atoms and increasing of the ΔpK_a values. Another trend was observed for compounds **2**–**5**, where the melting points decreases with decreasing electronegativities of the halogen atoms and increasing of the ΔpK_a. The exception is the compound **5**, for which the melting point is the highest among the co-crystals formed from acridine and *ortho*-halobenzoic acids, while the ΔpK_a is one of the largest. All of this is a result of the differences in the number, type and strength of intermolecular interactions occurring in the crystals of the title compounds (Table 5). Thus, the total numbers of C–H···O and C–H···π hydrogen bonds in compounds **2**–**5** are similar. However, the number of all C–H···X hydrogen bonds decreases with the size of the halogen atom and are 6, 4, 4 and 2 for co-crystals **2**–**5** respectively. Analysis of the intermolecular halogen bonds in the co-crystals formed from acridine and *ortho*-halobenzoic acids shows that strong I24···O22 [*d*(I···O)=3.26 Å], and F24···F25 halogen bonds [*d*(F24···F25) = 2.81 Å], much shorter than the sum of the van der Waals radii of iodine and oxygen atoms (3.50 Å) and fluorine atoms (2.94 Å), occurs in the co-crystal of **5** and **2**, respectively. In the crystal packing of compounds **3** and **4,** no X···O and X···X halogen bonds are present, which clearly explains why compounds **2** and **5** have the highest melting point among compounds **1**–**5**. Comparison of the melting points of compounds **2**–**4** shows that acridine • 2-fluoroobenzoic acid co-crystals melt at a higher temperature than the co-crystals of acridine • 2-chloro- and 2-bromobenzoic acids. The reason is that a disordered fluorine atom participates in the above mentioned F···F halogen bond, and C–H···F interactions (shorter than the sum of the van der Waals radii H and F atoms, 2.67 Å) between 2-fluorobenzoic acid molecules, and 2-fluorobenzoic acid and acridine molecules in **2**. In turn, the disordered chlorine and bromine atoms are involved only in one, weak C–H···X hydrogen bond between halobenzoic acid and acridine molecules in **3** and **4** respectively. The reason why the acridine • 2-chloroobenzoic acid co-crystal melts at a higher temperature than the isostructural co-crystal of acridine • 2-bromobenzoic acid may be that C–H···X hydrogen bonds are stronger in the former.

Table 5 The number of hydrogen bonds, halogen bonds and melting points in the title compounds.

Compound	No. of O–H···N hydrogen bonds	No. of C–H···O hydrogen bonds	No. of C–H···π hydrogen bonds	No. of C–H···X hydrogen bonds	No. of X···X halogen bonds	No. of X···O halogen bonds	m.p. of co-crystal /°C	m.p. of acid[a] /°C
1	1	3	2	-	-	-	94.7	123.3
2	1	4	2	6	1	-	99.0	125.5
3	1	3	1	4	-	-	95.5	140.8
4	1	3	1	4	-	-	93.5	149.6
5	1	4	-	2	-	1	99.3	163.3
6	1	3	-	4	-	1	122.9	124.6
7	1	3	-	3	-	1	129.5	154.8
8	1	3	-	3	-	1	137.3	158.5
9	1	3	-	3	-	1	140.2	188.2

[a] measured under the same conditions as co-crystals; the melting point of acridine is 100.8 [°C].

In the case of compounds **6**–**9**, the melting points increase with increasing strength of the X···O halogen bond between the halogen atom and the oxygen atom of the carboxyl group. Even though the co-crystals of **6**–**9** are isostructural, and the same number and type of interactions occur in their crystal packing, X24···O22 distances (3.30, 3.40, 3.42 and 3.47 Å for compounds **6**–**9**, respectively) are longer by about 0.31, 0.13 and 0.05 Å in compounds **6**, **7** and **8** respectively, and shorter by about 0.03 Å in compound **9** than the sum of the van der Waals radii of the X and O atoms. An investigation of the intermolecular interactions occurring in the crystals of the *ortho*-halobenzoic acids (the CSD refcodes: FBENZA01, CLBZAC01, BRBZAC01, OIBZAC01) shows that π–stacked columns of halobenzoic acids molecules are formed in all cases. The neighbouring columns are linked by C–H···X hydrogen bonds and the strength of these interactions weakens with decreasing electronegativities of the halogen atoms, which results in the H···X distances: 2.58, 2.99, 3.15 and 3.47 Å for 2-fluorobenzoic, 2-chlorobenzoic, 2-bromobenzoic and 2-iodobenzoic acid, respectively. Simultaneously, the strength of the X···X halogen bonds rises with increasing size of the substituent. In these interactions the distances between halogen atoms are *d*(F···F) = 4.63 Å; *d*(Cl···Cl) = 4.92 Å; *d*(Br···Br) = 4.09 Å; *d*(I···I) = 3.92 Å, and are longer by about 1.69, 1.42 and 0.39 Å in the crystals of 2-fluorobenzoic, 2-chlorobenzoic and 2-bromobenzoic acids respectively, and shorter by about 0.04 Å in the crystals of 2-iodobenzoic acid than the sum of the van der Waals radii of the X atoms. A similar tendency is observed for the *meta*-halobenzoic acids (the CSD refcodes: COVJIG, MCBZAC, MBBNZA, ZZZOAE01), where the H···X distances are 2.72, 3.15, 3.19, and 3.23 Å and the X···X distances are: *d*(F···F) = 3.15 Å; *d*(Cl···Cl) = 3.64 Å; *d*(Br···Br) = 3.84 Å; *d*(I···I) = 3.98 Å, and are longer by about 0.21, 0.14, 0.14 and 0.03 Å in the crystals of 3-fluorobenzoic, 3-chlorobenzoic, 3-bromobenzoic and 3-iodobenzoic acids, respectively, than the sum of the van der Waals radii of the X atoms. The X···O halogen bond is not observed in the crystals of examined halobenzoic acids. As a consequence, the melting points increase with increasing strength of the X···X halogen bond in the case of both *ortho*- and *meta*- halobenzoic acids. The above mentioned analyses confirm the general observation that complexes formed by iodo-substituted acids are halogen-bonded, whereas complexes of F-, Cl- and Br-substituted acids are hydrogen-bonded.[2–9]

Conclusions

Structural investigations of compounds obtained from the co-crystallization of acridine with nine benzoic acids show that proton transfer does not occur in any of these cases and that co-crystals are formed. The O–H···N hydrogen bonded heterodimers are linked by C–H···O hydrogen bonds and produce heterotetramers. The adjacent tetramers are linked by $\pi_{(acid)}$–$\pi_{(acid)}$ and C–H···O hydrogen bonds in **1**, and $\pi_{(acridine)}$–$\pi_{(acridine)}$ and by a C–H···X hydrogen bonds in compounds **2**–**5**. Additionally, the X···X and X···O halogen bonds occur in the co-crystal of **2** and **5**, respectively. In compounds **6**–**9**, the $\pi_{(acridine)}$–$\pi_{(acridine)}$ only interactions between neighbouring tetramers are observed. The adjacent π–stacked columns of acridine molecules formed in **2**–**9** are linked by C–H···$\pi_{(acid)}$ or C–H···X hydrogen bonds in **2**, C–H···O, C–H···$\pi_{(acid)}$ or C–H···X hydrogen bonds in **3** and **4**, and C–H···O, and C–H···X in **5**. In all the co-crystals formed from acridine and *meta*-halobenzoic acids, these columns interact by C–H···O hydrogen bonds; a C–H···X hydrogen bond is additionally observed in the crystal of **6**. The adjacent blocks observed in the crystal packings of these compounds are linked *via* C–H··$\pi_{(acridine)}$ interactions in **1** and C–H··$\pi_{(acid)}$, C–H···O and C–H···X hydrogen bonds in **2**. In the other compounds, the neighbouring blocks are linked by $\pi_{(acid)}$–$\pi_{(acid)}$, however, these interactions are accompanied by C–H···X hydrogen bonds and a X···O halogen bond in compounds **6**–**9**. The melting points of the co-crystals are in the following order: **4**<**1**<**3**<**2**<**5**<acridine<**6**<**7**<**8**<**9** and correlate with the number and strength of hydrogen bonds and halogen bonds observed in the crystal packings of the title compounds. Based on the above analysis, it can be concluded that the presence and strength of hydrogen and halogen bonds influence the melting points of the co-crystals formed from acridine and both *ortho*- and *meta*-halobenzoic acids.

Acknowledgements

This study was financed from the State Funds for Scientific Research through the National Science Centre in Poland, grant No. 2011/01/D/ST4/04943 (contract No. UMO-2011/01/D/ST4/04943).

This paper is dedicated to Professor Jerzy Błażejowski on his 70th birthday.

Notes

Faculty of Chemistry, University of Gdańsk, W. Stwosza 63, 80-308 Gdańsk, Poland.
**Corresponding author. E-mail: artur.sikorski@ug.edu.pl*
Tel.: +48 58 523 5112

† Electronic Supplementary Information (ESI) available: CIF files. CCDC 1047945-1047953. For crystallographic data in CIF or other electronic format, see DOI: 10.1039/b000000x/

References

1 (a) Desiraju, G. R. *Angew. Chem. Int. Ed. Engl.* **1995**, *34*, 2311.(b) Braga, D.; Grepioni, F. *Making Crystals by Design: Methods, Techniques and Applications*, **2007**, Wiley-VCH, Weinheim. (c) Aakeröy, C. B.; Desper, J.; Scott, B. M. T. *Chem. Commun.* **2006**, *13*, 1445.

2 (a) Aakeröy, C. B.; Baldrighi, M.; Desper, J.; Metrangolo, P.; Resnati, G. *Chem. Eur. J.* 2014, **19**, 16240. (b) Aakeröy, C. B.; Wijethunga, T. K.; Haj, M. A.; Desper, J.; Moore, C. *CrystEngComm*. 2014, **16**, 7218. (c) Aakeröy, C. B.; Panikkattu, S.; Chopade, P. D.; Desper, J. *CrystEngComm*, 2013, **15**, 3125. (d) Aakeröy, C. B.; Fasulo, M.; Schultheiss, N.; Desper, J.; Moore, C. *J. Am. Chem. Soc.* 2007, **129**, 13772.

3 (a) Mukherjee, A.; Tothadi, S.; Desiraju G. R. *Acc. Chem. Res.,* 2014, **47**, 2514. (b) Dubey, R.; Pavan, M. S.; Desiraju, G. R. (2012). *Chem.Commun*., 2005, **48**, 9020. (c) Mukherjee, A.; Desiraju, G. R. *IUCr*, 2014, **1**, 49.(d) Tothadi S.; Desiraju G. *Chem. Commun.*, 2013, **49**, 7791.

4 (a) Awwadi, F. F.; Willett, R. D.; Peterson, K. A.; Twamley, B. *Chem.-Eur J.* 2006, **12**, 8952. (b) Awwadi, F. F.; Taher, D.; Haddad, S. F.; Turnbull, M. M. *Cryst. Growth Des.*, 2014, **14**, 1961. (c) Awwadi, F. F.; Willett, R. D.; Twamley, B. *J. Mol. Struct.*, 2009, 918, 116.

5 (a) Takemura, A.; McAllister, L. J;, Karadakov, P. B.; Pridmore, N. E.; Whitwood, A. C.; Bruce, D. W. *CrystEngComm*, 2014,**16**, 4254. (b) Takemura, A.; McAllister, L. J.; Hart, S.; Pridmore, N. E.; Karadakov, P. B.; Whitwood, A. C.; Bruce, D. W. *Chem. Eur. J.*, 2014, **20**, 6721.

6 Ding, H. ; Lu, Y. ; Wu, W. ; Liu, H. *Chem. Phys.*, 2014, **441**, 30.

7 Podsiadło, M.; Olejniczak, A.; Katrusiak, A. *CrystEngComm*, 2014, **16**, 8279.

8 Santos-Contreras, R.J.; Martínez-Martínez, F.J.; Mancilla-Margalli, N.A.; Peraza-Campos, A.L.; Morín-Sánchez, L.M.; García-Báez, E.V.; Padilla-Martínez, I.I. *CrystEngComm*, 2009,**11**,1451.

9 Durka, K.; Luliński, S.; Jarzembska, K.N.; Smętek, J.; Serwatowski, J.; Woźniak, K. *Acta Cryst.*, 2014, **B70**, 157.

10 The CSD refcodes: (a) AFERAG, CEKLAH, CEKNAJ, CEVGUF, FBENZA, FBENZA01, FBENZA02, HANHEL, MEDBII, OCIQEX, TUDLOT, VAQRUB. (b) CLBZAC, CLBZAC01, CLBZAC02, ALOQIC, CEKMUC, DEZZUF, EXEZEN, EXIBIX, GEPMAR, IVUKIU, IVUKOA, JAMYEC, KDHOBC, KOFCUE, MEDBOO, NEBVOH, ONAPUP, PEQHOJ, ROFLOP, TOJFUU, WIDWIP, ZUSMEF, ZZZUMI. (c) BRBZAC, BRBZAC01, CEKMOW, DIBBAT, FEPQIA, GEPKOD, JAMYUS, PEQJEB. (d) HIMXIC, LSDIBZ, LDSIBZ01, OIBZAC, OIBZAC01. (e) AFEQUZ, CACGUK, CEKLUB, CEKNOX, COVJIG, COVJIG01, HOLJAU, HOLJAU01, HOLJAU02, HOLJAU03, HOLJAU04, HOLJAU05, HOLJAU06, HOLJAU07, IVULER, IVULIV, LATDOB, MEDCEF, VAQTEN. (f) VOJXUB, XONQIC, ALOQOI, AQAGEF, CEKLOV, EDUWOP, ELUPEH, GEPMEV, HUKHEP, HURMOW, HURMUC, IVUQOG, IVUQUM, JAMYAY, KHCBZO10, KHCBZO11, LENEV, MACJEG, MBZAC01, MBZAC, MEDCIJ, MEXDEA, OCEMUG, PEQHID, POYXOR, ROKQEN, RIJQET, SECXIJ, VAQSAI, VAQTOX, XIVDAJ, YUQKUR, ZUSMOP, ZUSMUV. (g) VOJYAW, CEKLIP, GEPJUI, HUKHOL, JAMYOM, MBBNZA, PEQJAX, QQQAFP. (h) VOJYUQ, FIWREJ, KOBGIS, KOFMUO, KOFNAV, MOKVAK, QQQAFG, SIXBAD, TOHXOE, TOHXUK, TOHYAR, TOHYEV, TOHYIZ, ZZZOAE, ZZZOAE01, ZZZOAE02.

11 (a) Sikorski, A.; Trzybiński, D. *Tetrahedron Lett.*, 2014, **55**, 2253. (b) Sikorski, A.; Trzybiński, D. *J Mol. Struct*., 2013, **1049**, 90.

12 (a) Sikorski, A.; Trzybinski D. *Tetrahedron Lett.*, 2013, **54**, 1463. (b) Lemmerer, A.; Adsmond, D. A.; Bernstein J. *Cyst. Growth Des.* 2011, **11**, 2011. (c) Aghabozorg, H.; Goodarzi, S.; Mirzaei, M.; Notash B. *Acta Cryst.*, 2011, **E67**, o126. (d) Eshtiagh-Hosseini, H.; Hassanpoor, A.; Mirzaei, M.; Salimi A. R. *Acta Cryst.*, 2010, **E66**, o2996. (e) Derikvand, Z.; Aghabozorg, H.; Gharamaleki J. A. *Acta Cryst.*, 2009, **E65**, o1173. (f) Mei, X.; Wolf, C. *Eur. J. Org. Chem.*, 2004, 4340. (g) Shaameri, Z.; Shan, N.; Jones W. *Acta Cryst.*, 2001, **E57**, o945.

13 (a) CrysAlis CCD and CrysAlis RED, Oxford Diffraction Ltd, Yarnton, England, Version 1.171.36.24 (2012). (b) Sheldrick G. M. *Acta Crystallogr,* 2008, **A64**, 112. (c) Spek A. L. *Acta Crystallogr.* 2009, **D65**, 148.(d) Johnson C. K. ORTEP II, Report ORNL-5138, Oak Ridge National Laboratory, Oak Ridge, TN, USA, 1976. (e) Motherwell S.; Clegg S. PLUTO-78. *Program for Drawing and Molecular Structure*, University of Cambridge: UK, 1978. (f) Macrae C. F.; Bruno I. J.; Chisholm J. A.; Edgington P. R.; McCabe P.; Pidcock E.; Rodriguez-Monge L.; Taylor R.; van de Streek J.; Wood P. A. *J. Appl. Cryst.* 2008, **41**, 466.

14 (a) Haynes, W. M. Ed *CRC Handbook of Chemistry and Physics*, 2013, 94th Edition, CRC Press/Taylor and Francis, Boca Raton, FL. (b) www.zirchrom.com/organic.htm.

15 Jenniefer, S. J.; Muthiah, P.T. *Chem. Cent. J.*, 2014, **8**, 20.

16 (a) Cinčić, D.; Friščić, T.; Jones, W. *Chem. Eur. J.*, 2008, **14**, 747. (b) Cinčić, D.; Friščić, T.; Jones, W. *Chem. of Mater.*, 2008, **20**, 6623. (c) Orola, L.; Veidis, M. V.; Mutikainen, I.; Sarcevica, I. *Cryst. Growth Des.*, 2011, **11**, 4009. (d) Montis, R.; Hursthouse, M. B.; Chan, H. C. S.; Kendrick, J.; Leusen, F. J. J. *CrystEngComm*, 2012, **14**, 1672.